RESONANT MAGNETIC X-RAY SCATTERING FROM *IN SITU* GROWN HOLMIUM-METAL FILMS

C. Schüßler-Langeheine,[1] E. Weschke,[1] R. Meier,[1] A.Yu. Grigoriev,[1] H. Ott,[1] Chandan Mazumdar,[1] D.V. Vyalikh,[1] C. Sutter,[2] D. Abernathy,[2] G. Grübel,[2] G. Kaindl[1]

[1]Institut für Experimentalphysik, Freie Universität Berlin
Arnimallee 14, D-14195 Berlin-Dahlem, Germany

[2]European Synchrotron Radiation Facility
B.P. 220, F-38043 Grenoble Cedex, France

Abstract

Resonant magnetic X-ray scattering (RMXS) experiments at the Ho-L_3 and M_5 thresholds have been performed on thin holmium-metal films grown *in situ* in ultra-high vacuum on W(110). The experimental set-up for these experiments as well as results for the magnetic structure of these films will be described. The magnetic structure stays bulk-like down to a thickness of 14 monolayers.

Introduction

Ultra-thin metal films are currently the subject of intense studies, not only because of their technological relevance but also because their properties are interesting from a fundamental point of view. The electronic structure of thin films can be different from that of bulk samples because the translational symmetry is lifted in one direction leading, e.g. to standing electron waves, which reveal details of the potential in the material [1]. Also, the magnetic properties of thin films can be altered relative to the bulk, e.g. due to shape anisotropy [2], strain [3] and finite-size effects [4]. Thin-film samples are either grown *ex situ*, usually by molecular-beam epitaxy (MBE), and transferred to the measuring chamber or grown *in situ* in the measuring chamber itself. One advantage of the latter procedure is that no protective cap layers are needed to prevent the samples from oxidation during transfer. Furthermore, samples grown *in situ* can be probed by surface-sensitive techniques, like photoelectron spectroscopy (PES) or scanning tunnelling microscopy (STM), giving access to the electronic structure and surface morphology.

A well-suited technique for the study of structural and magnetic properties of thin films is X-ray scattering, probing the electron distribution [5] as well as the spin and angular momentum distribution [6]. The probing depth for hard X-rays is of the order of a few μm, well adapted to the dimensions of thin films. Furthermore, the resonant enhancement of the scattering cross-section at the absorption thresholds can be used to perform element-selective measurements [6-8]. One of the prototype materials for resonant magnetic X-ray scattering (RMXS) is Ho metal [7-9] because the open 4*f* shell in Ho carries the strongest magnetic moment among all elements, and Ho is anti-ferromagnetic over a wide temperature range with the magnetic scattering signal well separated from that of charge scattering. The Ho L_3 resonance at 8 074 eV corresponds to a photon wavelength of 1.54 Å, well suited for structural studies. The helical anti-ferromagnetic structure in Ho consists of ferromagnetically ordered moments in the basal planes of the *hcp* lattice with each plane rotated by a certain angle with respect to the neighbouring plane, thus forming a helix along the crystallographic *c* axis [10]. In this contribution, we report on resonant magnetic X-ray scattering experiments performed on epitaxial Ho-metal films grown *in situ* on W(110) at the Ho L_3 threshold in the hard and the M_5 threshold in the soft X-ray range, where films of thickness of only a few monolayers (ML) can be studied.

Experimental

For the experiments, two different UHV diffractometer set-ups were designed adapted to the hard and soft X-ray regions, respectively. For hard X-rays, a vacuum chamber made from a modified commercial CF100 double-cross was built, small enough to fit onto common diffractometers. For the incoming and outgoing photons, two UHV-compatible Be windows of about 0.5 mm thickness were used. The chamber was pumped by a turbomolecular pump backed by an oil-free turbo/diaphragm pump combination. Together with a Ce sublimation pump and with the closed-cycle He refrigerator for sample cooling in operation, vacuum in the 5×10^{-11} mbar range was readily achieved. For film preparation, the chamber was equipped with a quartz-microbalance thickness monitor and a quadrupole mass spectrometer for residual-gas analysis. The chamber could be mounted in different orientations allowing both horizontal and vertical scattering geometries. The weight of the whole set-up was about 70 kg, but the load on the diffractometer could be further reduced by a counterbalance. The set-up was successfully installed at the ID10A (Troïka 1) beam line of the ESRF, where the hard X-ray data shown in this contribution were recorded, at the HASYLAB W1.1 beam line, and also on a laboratory diffractometer. Since for the soft X-ray range around the lanthanide $M_{4,5}$ thresholds no suitable window material is available, a second set-up was built, where the sample and the detector could be moved inside an UHV chamber that was directly attached to the beam line. Since the limitations concerning size and weight of the set-up do not apply here, a conventional, fully-equipped vacuum

chamber could be used in this case. A silicon-diode detector behind an adjustable rectangular slit was mounted on an arm, which could be rotated in vacuum. The sample was mounted on a second rotational feedthrough with the rotational axes of sample and detector aligned. The necessary mechanical precision was readily achieved in UHV, since at the larger wavelengths in the soft X-ray region, the requirements concerning angular resolution are more relaxed and the diffraction features move to comparably larger angles. The angular resolution was of the order of 0.1°. The soft X-ray data presented here were recorded at the U49/1-SGM beam line of BESSY II.

Both experimental set-ups were equipped with the same sample holder, W(110) substrate crystal, and with identical home-built evaporators. The substrate crystal was held in a Ta frame attached via a sapphire plate to a closed-cycle refrigerator. The sample could be heated by a filament situated at the back side of the substrate crystal either irradiatively or by electron bombardment. This design allowed to cover a temperature range of the sample from 30 K up to ~2 000 K, which is needed to desorb a film from the substrate surface. The temperature was determined by a carefully calibrated $W_{0.95}Re_{0.05}$/ $W_{0.74}/Re_{0.26}$ thermocouple attached in a small hole in the substrate crystal with the thermocouple wires led without interruption to a commercial temperature controller.

Ho metal was evaporated from an evaporation cell that consisted of a doubly-shielded Ta crucible and that was heated by electron bombardment. During evaporation, the pressure rose to about 5×10^{-10} mbar. The growth and annealing process could be monitored *in situ* via the X-ray reflectivity [11,12] as shown in Figure 1 for the case of a 77-Å thick Ho film.

Figure 1. Ho film preparation

The upper curve shows the X-ray reflectivity during the process, the lower curve represents the corresponding sample temperature; see text for details

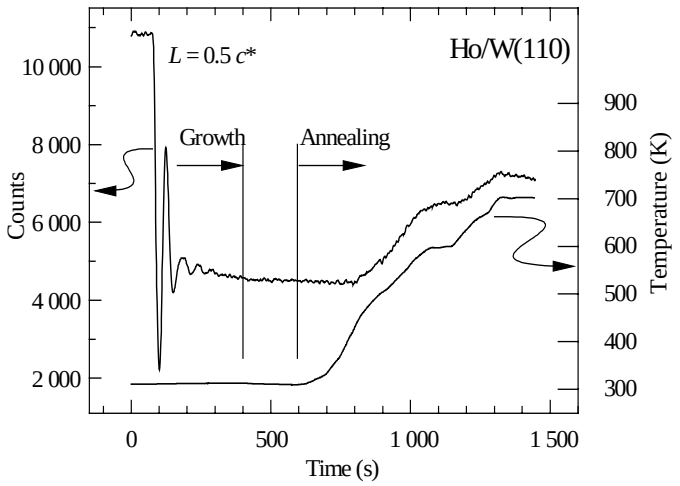

The data were taken in specular geometry at a photon energy of 8 074 eV, with the length of the scattering vector, L, given in units of the Ho reciprocal lattice vector, c^*. In this notation, $L = 2c^*$ corresponds to the Bragg condition for the close-packed planes. The upper curve displays the X-ray reflectivity as a function of time and the lower curve the temperature. The film was grown with the substrate kept at room temperature; the high reflectivity in the beginning stems from the clean W substrate. After the shutter of the evaporator was opened, the reflectivity dropped and damped growth oscillations were observed. For the case of heteroepitaxial growth, one oscillation corresponds to $2c^*/L$ double layers (because in an *hcp*-lattice c refers to the double-layer spacing) [11], i.e. four layers per oscillation in the present case. The damping of the oscillations is caused by an increasing

roughness of the film. Upon annealing, the reflectivity increases indicating a smoothening of the film. At about 710 K, the reflectivity starts to decrease, which is a signature of a re-entrant roughening, probably caused by a breaking of the film and islands formation, as observed for Gd/W(110) at about the same temperature [13]. Because in most cases multiple-scattering is not important for X-rays, the analysis of X-ray scattering data can often be performed within a simple kinematic theory. For the case of growth oscillations of Ho and Yb metal on W(110), details in the shape of the curves could be analysed taking relaxations of the interface layers during the growth of the first film layers into account [12]. Hence, beyond the obvious advantage of monitoring film thickness and annealing processes, *in situ* X-ray scattering allows access to the growth dynamics of the film. Lanthanide metal films grown in this way in UHV are characterised by a mosaic width of the order of 0.04°, i.e. they represent high-quality samples for magnetic structure studies.

Results

RMXS data from a 113-ML Ho film at various temperatures are shown in Figure 2. The charge contribution was suppressed by polarisation analysis using a graphite(006) analyser crystal [9]. The curves are still dominated by the charge-scattering Bragg peak at $L = 2c^*$ leaking through the analyser. The Bragg peak has the broad Laue shape with side oscillations because of the small number of scattering planes [5]. At low temperatures, two satellites caused by the magnetic superstructure are visible on both sides of the Bragg peak, offset by the magnetic modulation wave vector, τ. At 41 K, $\tau = 0.2\ c^*$, which corresponds to a bulk-like ten-layer magnetic period. Like in the bulk, τ is temperature dependent and the decreasing intensity of the satellite upon heating reflects the decaying magnetic order. A detailed analysis of the temperature dependence of τ and the satellite intensity reveals a high similarity to published bulk data, e.g. from Ref. [10] (see [14]). From the width of the magnetic satellite one can conclude that the whole film contributes coherently to the magnetic structure over the whole temperature range (see inset of Figure 2).

Figure 2. RMXS data from a 113-ML Ho/W(110) film at various temperatures

The data are taken at the Ho L_3 resonance with applied polarisation analysis in the $\sigma\pi$ channel. The inset shows the number of lattice planes contributing to the helical structure, N, as determined from the width of the (002-τ) satellite.

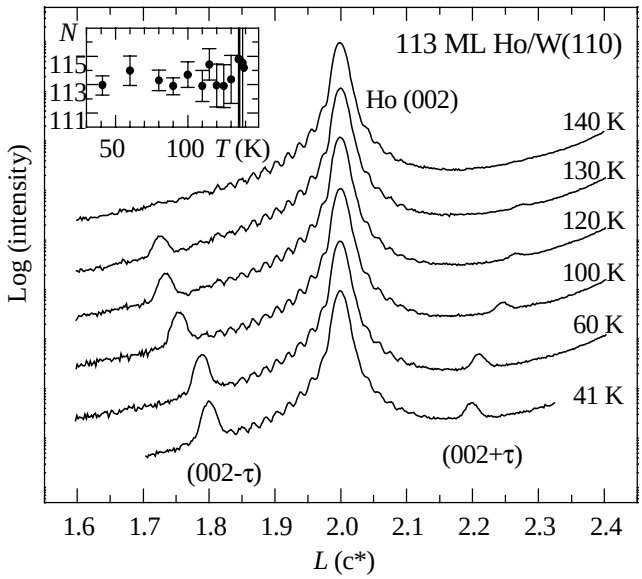

Since an Ho film of 113-ML thickness still behaves bulk-like, it is interesting to look at thinner films. Data from the thinnest film investigated so far using hard X-rays are shown in Figure 3. In the upper panel, the magnetic scattering signal (solid symbols) is plotted together with the charge scattering background (open symbols), which has been recorded with the polarisation analyser turned by 90° ($\sigma\sigma$-channel) [9] normalised to the same Bragg-peak height for both scans. The difference between the two curves, which represents the magnetic contribution, is shown in the lower panel on a linear scale. The magnetic satellite is clearly visible, and the magnetic modulation wave vector is the same as in the bulk. A detailed analysis of the temperature dependence, however, is not possible because of the strong charge-scattering background at the position of the satellite. The signal-to-background ratio will get even worse for thinner films because the satellite intensity is proportional to the squared number of layers whereas the increasing width of the charge-scattering Bragg peak leads to an essentially thickness-independent background height at the satellite position.

Figure 3. Upper panel: RXMS from a 33-ML Ho film in the charge-scattering ($\sigma\sigma$, open symbols) and in the magnetic-scattering ($\sigma\pi$, filled symbols) channel. Lower panel: The difference between the two upper curves on a linear scale.

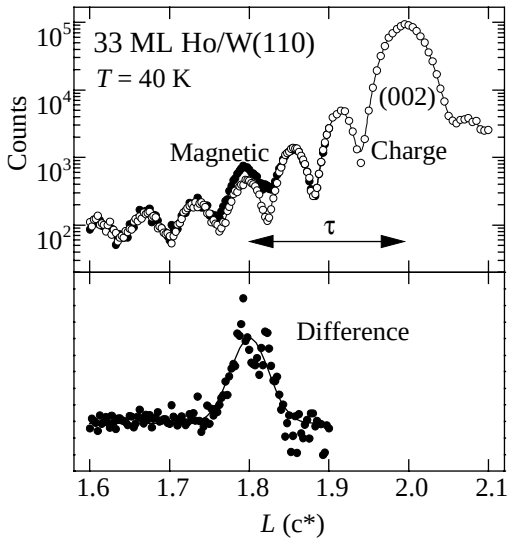

The situation is more favourable in the soft X-ray region. At the Ho M_5 threshold, where dipole excitations involve the shallow 4*f* states, which carry the magnetic moments, the resonant enhancement of the magnetic scattering cross-section is about 6 orders of magnitude [8,15] and thus much higher than the 50-fold enhancement at the L_3 threshold [7]. Even though the photon wavelength of about 9.2 Å at this energy is too large to allow a study of the crystal structure, it is well suited for the more extended magnetic structure of Ho metal. The (000+τ) magnetic satellite can be readily observed. Data taken from a 14-ML thick Ho metal film at the M_5 resonance are presented in Figure 4. The upper panel shows the reflectivity recorded at 40 K in the helical phase and at 180 K, well above the Néel temperature, respectively. The high-temperature data show pronounced oscillations which are caused by the interference between X-rays scattered at the film surface and the film-substrate interface [16]. At low temperatures, additional intensity appears, which represents the magnetic contribution. The corresponding difference is plotted in the lower panel. The magnetic satellite is again clearly visible having the same Laue shape as the Bragg peak. Even though the main maximum cannot be seen in all detail because of total reflection and footprint effects, its position is fully determined by the well-resolved side maxima (Laue oscillations). The value obtained for the satellite position (arrow in Figure 4) is $\tau = (0.2 \pm 0.04)c^*$, which is again the bulk value.

Figure 4. Reflectivity from a 14-ML thick Ho film measured at the M_5 resonance

Upper panel: Data recorded above (open symbols) and below (filled symbols) the Néel temperature. The difference, plotted in the lower panel, is the magnetic contribution, i.e. the (000+ τ) satellite (arrow) with two of the magnetic Laue oscillations visible.

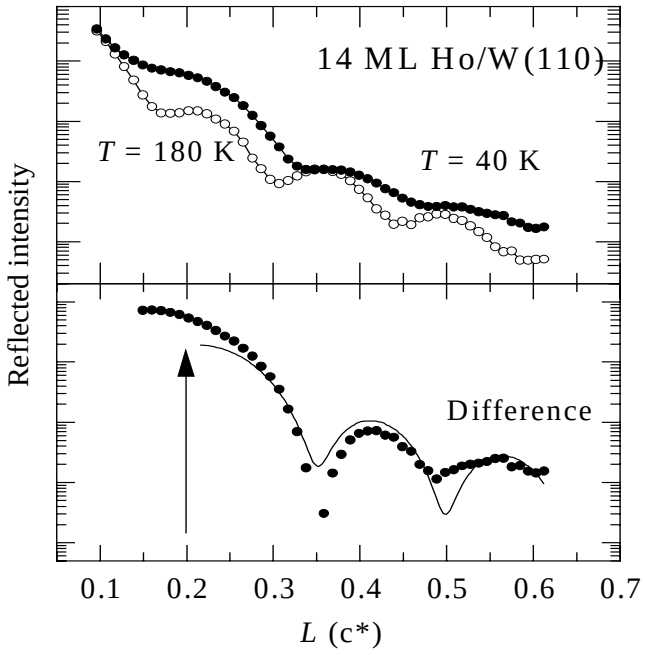

Discussion

Ho-metal films grown on W(110) exhibit a bulk-like magnetic structure down to thicknesses of at least 14 ML. This is quite surprising because the interaction responsible for the anti-ferromagnetic coupling is of long-range character. In a mean-field calculation for a 15-ML slab of Ho metal by Bohr, *et al*., the outermost three layers on each side of the slab are predicted to be ferromagnetically ordered due to their reduced number of neighbours [17]. Such a behaviour, which would lead to a substantial broadening of the magnetic satellite, is not observed in our data. Our method, however, is not sensitive to a ferromagnetic contribution caused by a canting of the moments out of the basal planes by a certain angle, like in the ferromagnetic low-temperature phase of bulk Ho metal.

Interesting results concerning the influence of cap layers and the kind of substrate material on the sample can be inferred from a comparison of the present results for on uncovered 14-ML film with those for a ≈16-ML Ho film sandwiched between two Y layers studied by neutron scattering by Leiner, *et al*. [18]. In contrast to our results, the authors of the neutron-scattering study find the helix period distinctly shorter than in the bulk with the coherence length of the helix almost twice as long as the thickness of the Ho film, probably due to the fact that the helix is continued in the polarisable Y metal layers.

Whereas the investigation of ultra-thin films is not feasible in the hard X-ray region due to the high charge-scattering background, it is quite possible at the M_5 resonance because of the strong resonant enhancement of the magnetic-scattering cross-section at this threshold. Soft X-ray scattering experiments are not only restricted to lanthanide metals. Strong magnetic scattering signals have been observed at the Fe-L_3 [19] and the uranium $M_{4,5}$ thresholds [20,21]. For actinide systems, the

wavelengths at the $M_{4,5}$ resonances are short enough to reach charge-scattering peaks and thus to correlate structural and magnetic properties. The *in situ* preparation method is not only restricted to metal films but has also been successfully applied for the preparation of, e.g. graphite-intercallation compound [22] and alloy films [23].

Summary

The anti-ferromagnetic structure of Ho-metal films grown *in situ* on W(110) has been investigated by resonant magnetic X-ray scattering at the L_3 and M_5 resonances. The much stronger resonant enhancement in the latter case allows to investigate films down to a thickness of only a few monolayers. Films in the thickness range from 14 to 113 ML show a bulk-like magnetic structure, in contrast to theoretical predictions, at least for the thinnest film studied here. From a comparison with the results of a recent neutron-scattering study of a 16-ML thick Ho film sandwiched between Y layers, the strong influence of cap layers and/or of the kind of the substrate materials can be inferred.

Acknowledgements

The authors are indebted to the staff of BESSY II for their co-operation in the preparation and performance of the experiments at the U49/1-SGM. This work was supported by the BMBF, project 05 SF8 KEC8, the DFG, Sfb290/TP A06, and the European Union (EFRE). C.M. acknowledges support from the Alexander von Humboldt foundation.

REFERENCES

[1] J.J. Paggel, T. Miller, T-C. Chiang, *Science*, 283, 1709 (1999).

[2] A. Pang, A. Berger, H. Hopster, *Phys. Rev. B*, 50, 6457 (1994).

[3] M. Hong, R.M. Fleming, J. Kwo, L.F. Schneemeyer, J.V. Waszcak, J.P. Mannaerts, C.F. Majkrzak, D. Gibbs, J. Bohr, *J. Appl. Phys*., 61, 4052 (1987).

[4] M. Farle, K. Baberschke, U. Stetter, A. Aspelmeyer, F. Gerhardter, *Phys. Rev. B*, 47, 11571 (1993).

[5] B.E. Warren, "X-ray Diffraction", Addison-Wesley Publishing Company, Reading (1969).

[6] M. Blume, *J. Appl. Phys*., 57, 3615 (1985).

[7] D. Gibbs, D.R. Harshman, E.D. Isaacs, D.B. McWhan, D. Mills C. Vettier, *Phys. Rev. Lett*., 61, 1241 (1988).

[8] J.P. Hannon, G.T. Trammell, M. Blume, D. Gibbs, *Phys. Rev. Lett*., 61, 1245 (1988).

[9] D. Gibbs, M. Blume, D.R. Harshman, D.B. McWhan, *Rev. Sci. Instrum*., 60, 2990 (1994).

[10] G. Helgesen, J.P. Hill, T.R. Thurston, D. Gibbs, J. Kwo, M. Hong, *Phys. Rev. B.*, 50, 2990 (1994).

[11] E. Weschke, C. Schüßler-Langeheine, R. Meier, G. Kaindl, C. Sutter, D. Abernathy, G. Grübel, *Phys. Rev. Lett*., 79, 3954 (1997).

[12] E. Weschke, C. Schüßler-Langeheine, R. Meier, G. Kaindl, C. Sutter, G. Grübel in *Advances in Solid State Physics*, B. Kramer, ed., p. 541, Vieweg Braunschweig (1999).

[13] A. Aspelmeier, F. Gerhardter, K. Baberschke, *J. Magn. Magn. Mater*., 132, 22 (1994).

[14] C. Schüßler-Langeheine, E. Weschke, A.Yu. Grigoriev, H. Ott, R. Meier, D.V. Vyalikh, C. Mazumdar, C. Sutter, D. Abernathy, G. Grübel, G. Kaindl, *J. Electron. Spectrosc. Relat. Phenom*. (in print 2000).

[15] E. Weschke, A.Yu Grigoriev, C. Schüßler-Langeheine, R. Meier, G. Kaindl, in preparation.

[16] L.G. Parratt, *Phys. Rev*., 95, 359 (1954).

[17] J. Bohr, D. Gibbs, J.D. Axe, D.E. Moncton, K.L. D'Amico, D.F. Majkrzak, J. Kwo, M. Hong, C.L. Chien, J. Jensen, *Physica B*, 159, 93 (1989).

[18] V. Leiner, D. Labergerie, R. Siebrecht, C. Sutter, H. Zabel, *Physica B*, 283, 167 (2000).

[19] H.A. Dürr, E. Dudzik, S.S. Dhesi, J.B. Goedkoop, G. van der Laan, M. Belakhovsky, C. Mocuta, A. Marty, Y. Samson, *Science*, 284, 2166 (1999).

[20] E.D. Isaacs, D.B. McWhan, C. Peters, G.E. Ice, D.P. Siddons, J.B. Hastings, C. Vettier, O. Vogt, *Phys. Rev. Lett*., 62, 1671 (1989).

[21] G.M. Watson, D. Gibbs, G.H. Lander, B.D. Gaulin, L.E. Berman, Hj. Matzke, W. Ellis, *Phys. Rev. B*, 61, 8966 (2000).

[22] S. Danzenbächer, S.L. Molodtsov, J. Boysen, Th. Gantz, C. Laubschat, A.M. Shikin, S.A. Gorovikov, M. Richter, *Physica B*, 259-261, 1153 (1999).

[23] W. Schneider, S.L. Molodtsov, M. Richter, Th. Gantz, P. Engelmann, C. Laubschat, *Phys. Rev. B*, 57, 14930 (1998).